Indian Journal of Geo Marine Sciences
Vol. 50 (12), December 2021, pp. 1066-1078

Mineral paragenesis and stratigraphic setting of the Neoproterozoic volcano-sedimentary succession of Samran Group, Jabal Farasan Area, West central Arabian Shield, Saudi Arabia

A A Mesaed*[a,b] & A R Sonbul[c]

[a]Geo-Exploration Techniques Department, Faculty of Earth Sciences, King Abdulaziz University, Jeddah, Saudi Arabia

[b]Geology Department, Faculty of Sciences, Cairo University, Giza, Egypt

[c]Engineering and Environmental Geology Department, Faculty of Earth Sciences, King Abdulaziz University, Jeddah, Saudi Arabia

*[E-mail: alimesaed@yahoo.com]

Received 30 October 2020; revised 07 December 2021

Jabal Farasan is located in the west central part of the Arabian Shield. The present study aims to reveal the stratigraphic setting and mineral paragenesis of the exposed volcano-sedimentary succession of the Samran Group in Jabal Farasan area. The succession of Samran Group is composed of three successive facies: the lower interbedded andesitic tuffs and tuffaceous andesites and trachyte's (F1), the middle-altered quartz diorite/andesite (F2) and, an upper interbedded andesitic tuff, tuffaceous andesites and trachytes (F3). The vertical variations in the petrographic lithotypes depend mainly on the position of the depositional sites relative to the volcanic centers (proximal and distal). Both the volcanic rocks and the associated units are subjected to syn-and post-depositional diagenetic/metamorphic processes. These processes include the formation of the Fe^{2+}-silicates: (*i.e*., chlorite instead of the volcanic ashes and the formation of plagioclase minerals). Post diagenetic recrystallization of the tuffaceous mudstones and the formation of microcrystalline quartz. The diagenetic oxidation of the Fe^{2+}-silicates led to the formation of volcaniclastic red beds in certain stratigraphic horizons.

[**Keywords**: Arabian shield rocks, Jabal Farasan, Samran Group, Volcaniclastics]

Introduction

Wide classification schemes[1,2] are used for the description of volcaniclastic components *i.e.* pyroclastic and epiclastic fragments. The fragments formed by direct volcanic activity are suggested to be pyroclastic up to the point where they become refragmented following lithification, regardless of whether they have been reworked, their shape has been changed by transport processes or whether they have been lithified[1]. In pyroclastic fragments become epiclastic as soon as they have been reworked by surface (sedimentary) processes, even if this only involves rolling down a hillside in response to gravitational forces[2]. The Arabian Shield has been divided into western and eastern parts[3] (Fig. 1). The western part is made of four terrains of oceanic crust affinity. These terrains are Midyan, Hijaz, Jeddah and Asir. The eastern part of the Arabian Shield includes Khida, Afif, Ar-Rayn, Ad-Dawadimi and Hail terrains which are of continental crust affinity. The distribution of these terrains and the location of Jabal Farasan is shown in Figure 1(ref. 4). In the Precambrian Arabian Shield of Saudi Arabia, the layered successions consist of slightly metamorphosed (green schist and amphibolite facies) volcaniclastic successions. Most of the Cu, Ag, Pb, Zn and Au deposits of Saudi Arabia are enclosed within the old (oceanic) slightly metamorphosed volcaniclastic successions. Also, the marble deposits of Jabal Farasan (west central part of Saudi Arabia) present as intercalations within the volcaniclastic succession of the Samran Group.

Physiography and geologic setting

Samran group

The layered metamorphosed volcano-sedimentary succession and the marble bands at Jabal Samran are believed to be equivalent the Hulayfah Group of the Arabian Shield[5,6]. Samran Series was suggested to be composed from andesitic volcanics at the Jabal Samran area[7]. Samran Group was used instead of ''Samran series"[6]. The metabasalt to meta-andesite (Qirshah Formation) of Jeddah Group can be correlated with the ''Samran series"[9-11]. Jeddah Group represents an early stage of mafic and intermediate volcanism and volcaniclastic deposition of the Hijaz

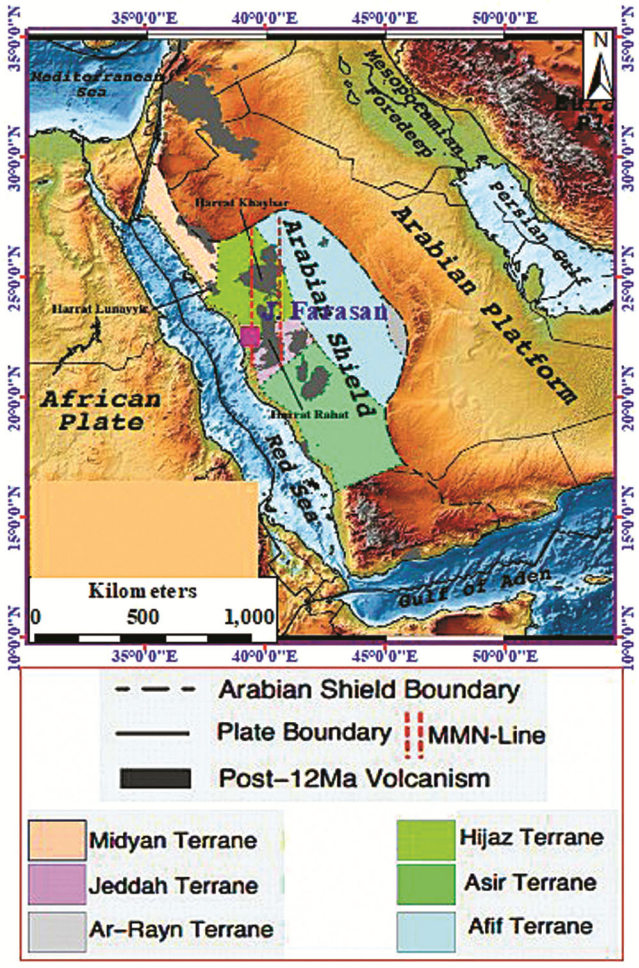

Fig. 1 — Geographic map of the Arabian plate and surrounding regions, showing also the major geologic features of six accreted terranes (Midyan terrane, Hijiaz terrane, Jeddah terrane, Asir terrane, Afif terrane and Ar Rayn terrane), and areas of volcanic activity in the last 12 million years[4]

tectonic cycle[12]. Jeddah and Samran groups are composed from metabasalt, meta-andesite and graphitic schists of the Baish-Bahah groups and has been formed during the early Hijaz cycle. They are suggested to be formed in subaerial to shallow marine environments and metamorphosed to upper greenschist facies[13]. An estimated 825 – 745 age for the Samran Group was assumed by Blodget & Brown[14]. Lateral and vertical facies variations led to the subdivision of the Samran Group into five formations (Nida, Shayban, Madrakah, Fayidah and Amudan)[15].

Aims and objectives

The present study aims to study the stratigraphic setting, petrography and mineral paragenesis of the volcaniclastic succession of the Samran group in Jabal Farasan area. The facies types and vertical and lateral facies changes within the studied succession are also aimed. The syn-and post depositional diagenetic alterations as well as the metamorphism are also illustrated.

Materials and Methods

The present study is detailed field-based works microscopic investigations. Satellite images, topographic and geologic maps of the study area are used in this study. Detailed stratigraphic section was measured within the exposed black volcaniclastic succession of Jabal Farasan area beneath the marble deposits. The lab works include: the preparation of polished slabs for megascopic description of the volcaniclastic sediments. Microscopic description; stratigraphic measurements and geologic maps using the different computer software *e.g.*, ArcMap, Corel Draw, Harvard Graphics and PowerPoint.

Geology of the study area

Jabal Farasan area was previously mapped within Rabigh geologic map where the marble-bearing unit in Jabal Farasan area as metabasalt, chert and marble (Birak Group)[16]. The map shows marble-bearing succession was described as pelagic basalt, limestone and chert[15] (Fig. 2). The study area contains Precambrian Arabian Shield rocks, Phanerozoic sedimentary rocks, and the overlying basalt (Harrat) and wadi deposits. The geologic map[14] revealed the presence of the following rock units (Fig. 2):

I. Unassigned neoproterozoic rocks

Unassigned neoproterozoic rocks were described by Pallister *et al.*[17] and Stern *et al.*[18] comprises gabbro and metagabbro with serpentinite-gabbro lenses along shear zones representing the Arabian Shield ophiolites.

II. Layered Cryogenian lithostratigraphic units

a. Birak group, > 805 Ma: (br) which includes greenschist-facies basaltic, andesitic, dacitic, and rhyolitic flows and pyroclastic rocks (agglomerate, lapilli tuff, and ash tuff), greywacke, marble, quartzite, and chert. Banded pale gray and white marble is conspicuous at Jabal Farasan.

b. Samran Group, 825-745 Ma: Nida, Shayban, Madrakah, Fayidah and Amudan are the different formations of Samran group. The northern two formations may represent laterally equivalent distal and proximal volcanic assemblages deposited around paleovolcanic centers[15]. Madrakah and Fayidah

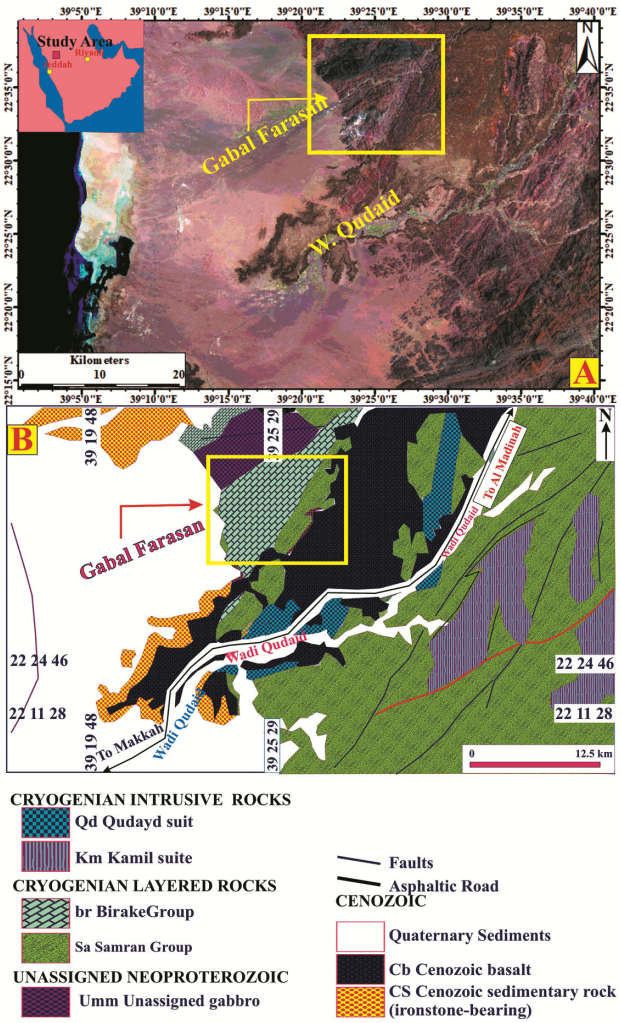

Fig. 2 — (A) Mr. Said Image of Jabal Farasan area; and (B) Detailed geologic map of Wadi Qudaid-Jabal Farasan[14]

represents a roof pendant in the Kamil suite. These two formations are assigned to the Samran group because of their proximity and general similarity to the other units[19]. The Amudan formation is a youngest formation.

III. Intrusive cryogenian lithostratigraphic units

1) Qudayd suite, 780-745 Ma (qd)[16] consists of elongated bodies of tonalitic orthogneiss that intrude the Samran group along the Bi'r Umq suture zone at the northern part of Jeddah. The gneiss has a well-developed, steeply dipping foliation and is cut by steeply dipping shear zones. Contacts are mostly steep, and the suite is concordant with the Samran group.

2) Kamil suite, 825-800 Ma (km)[16,19] consists of different types of plutonic rocks of calc-alkalic and locally trondhjemitic affinities in the southwestern part of the Jeddah terrane between the Bi'r Umq suture and the Makkah area. The suite intruding the deformed layered rocks of the Samran and Zibarah groups and plutonic rocks of the Makkah batholith.

Results

Physiography and geomorphology

Jabal Farasan represents a remarkable synform formed along major NE fault system. This major synform is intensively folded and faulted. It is affected by several NE major faults and represents the main site for marble in Saudi Arabia. In Jabal Farasan area, a well-preserved schistosity in the thick volcano-sedimentary succession is dominated.

The southeastern part of Jabal Farasan is developed along a major NE-fault. The contact line between the metamorphosed basic and intermediate volcanics and the associated volcaniclastics of Samara Group and the marble-bearing unit is present in the main NE wadi delineated by the main NE fault.

Measured section of the volcaniclastic succession

Field observations revealed that, the marble-bearing succession is composed mainly of thick units of basic volcanics, the intercalated volcaniclastics and marble. This succession is just overlying the green schist and amphibolites of the Samaran group within the northeastern and northwestern part of Jabal Farasan area. The stratigraphic succession was measured in the extreme SW part of Jabal Farasan. The measured section comprises ten stratigraphic units (Figs. 3, 4). The section represents successive and interlayered units of basic to intermediate volcaniclastics and carbonates. The legend of the measured section is present in Figure 4D. The Samran group attains up to 330 m and is composed mainly from dark basic to intermediate volcanics and the intercalated volcaniclastics (Figs. 3, 4). It is subdivided into three main facies F1, F2 and F3 (Table 1). Each of these facies was described in the field and their rocks were microscopically investigated and the results are given below:

Lower interbedded andesitic tuffs and tuffaceous andesites and trachyte F1

This facies attains up to 120 m thick and is composed of rhythmic alternations of greenish black and reddish-brown tuffs and tuffaceous andesite and trachyte (Fig. 5A). The detailed microscopic descriptions of the selected samples of these facies led to the recognition of seven petrographic lithotypes (Table 1). These petrographic lithotypes are described below as follows:

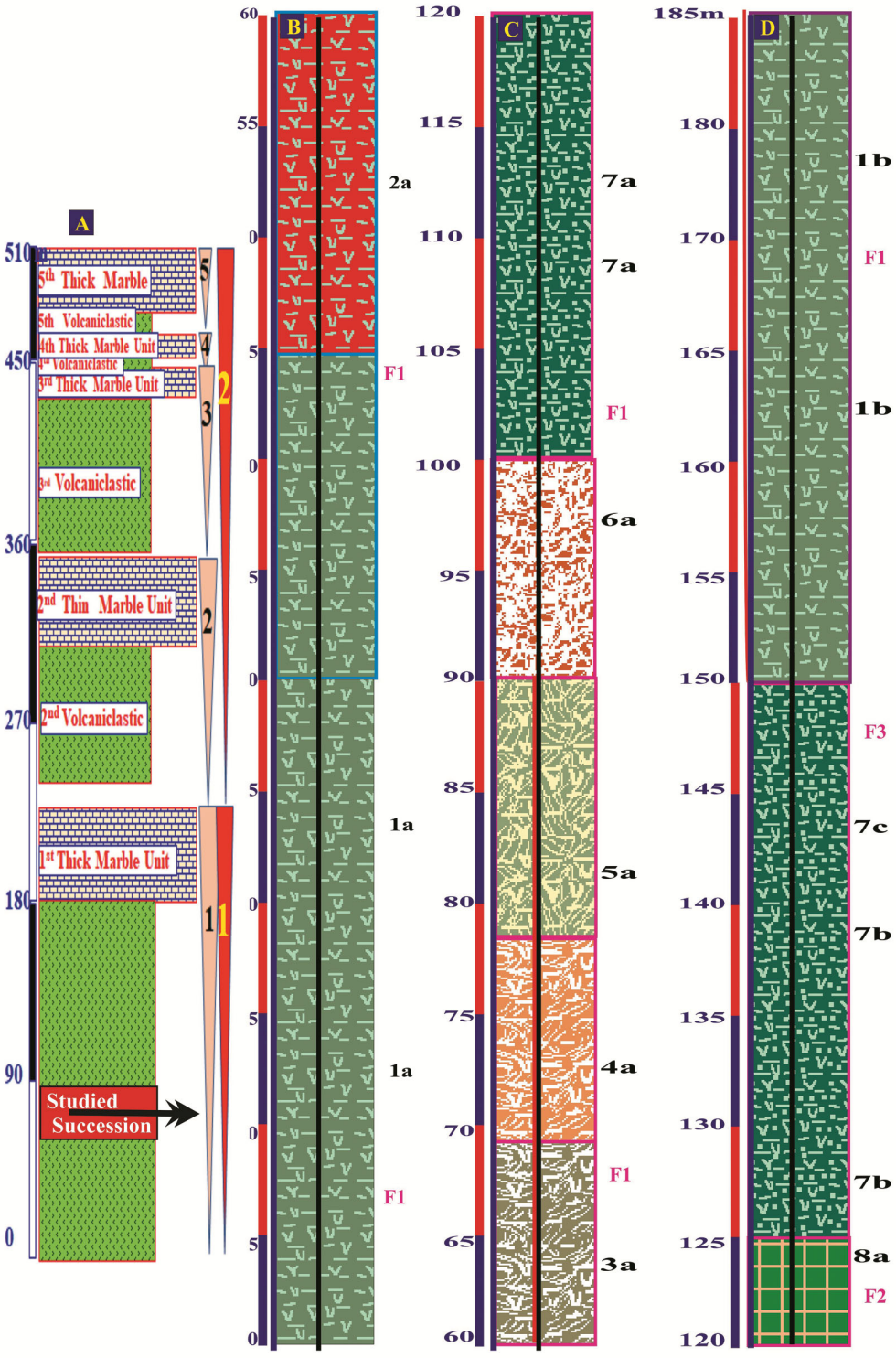

Fig. 3 — (A) The complete succession of Jabal Farasan area; and (B, C, D) The different facies of the lower and middle parts of the measured volcaniclastic succession of Samran Group, Jabal Farasan area

Chloritized and devitrified tuffs 1a

Chloritized and devitrified tuffs 1a occurs in the lower 50 m (Fig. 3, Column B) and it is represented by massive to slightly bedded reddish black to black tuffaceous mudstone. It consists mainly of thinly laminated light and dark green tuffaceous mudstone.

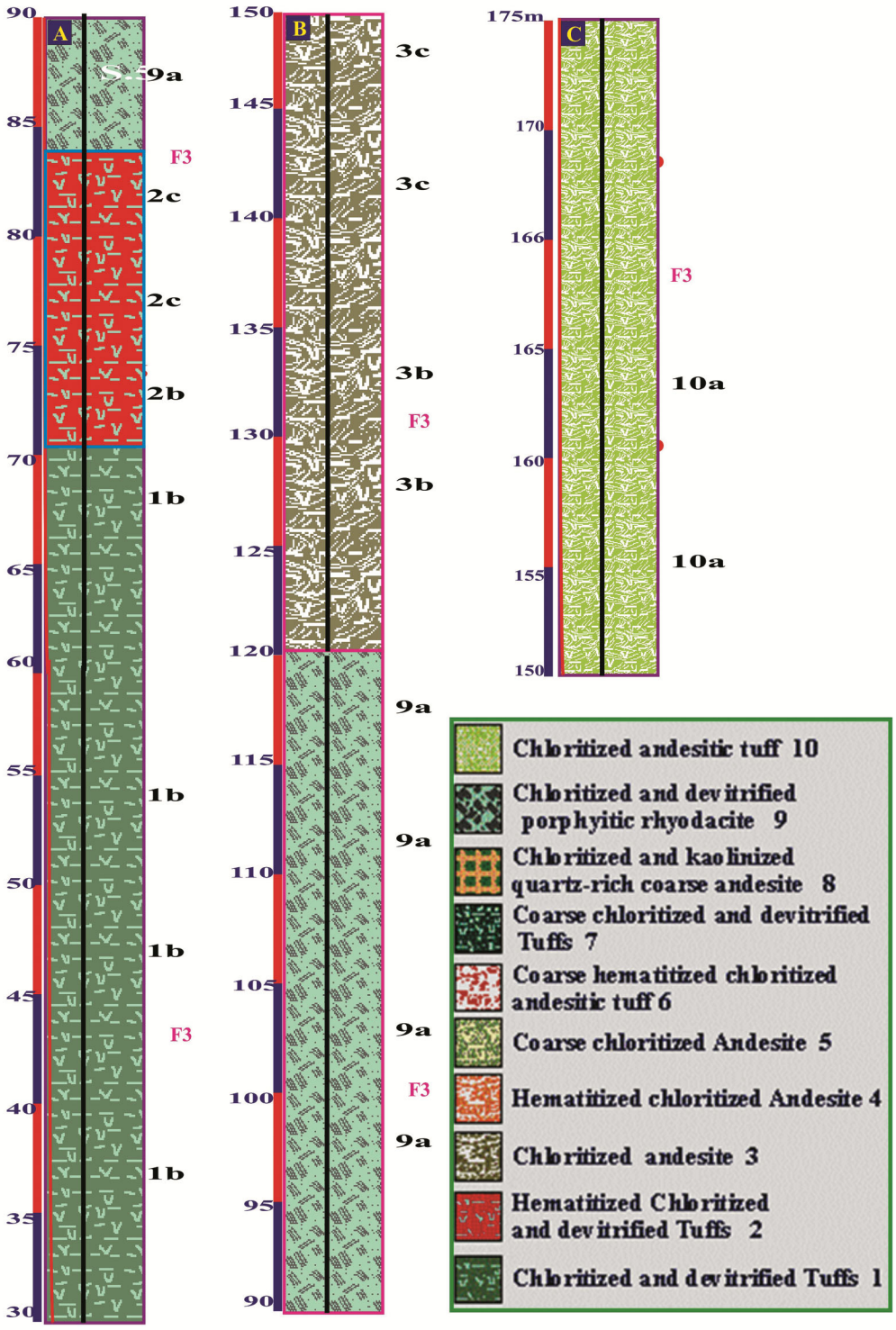

Fig. 4 — (A, B, C) The stratigraphic sections of the upper part of the volcaniclastic succession of Samran Group, Jabal Farasan area

The light green laminae are composed from devitrified tuffs that composed mainly from microcrystalline quartz. This type of bands shows the formation of light green chlorite flakes (Fig. 5B), giving a blue color for these bands between crossed nicols. The dark bands are dense and contain dark brown to black iron oxyhydroxides blotches formed instead of the chlorite flakes and domains.

Table 1 — The different Facies (F1, F2, F3) and related petrographic lithotype of Samran Group of Jabal Farasan area

Unit	Facies	Petrographic Lithotype
Studies succession of Samran Group (First Volcaniclastic Unit I of complete section of G. Farasan, column A of Fig. 3).	Upper Interbedded andesitic tuffs and tuffaceous andesites and trachytes F3	Chloritized Andesitic tuffs (Meta-tuff) 10a Chloritized Andesite (Meta-andesite) 3c Chloritized andesite 3b Hematitized Chloritized and devitrified Tuffs 2c Chloritized and devitrified Tuffs 1b Coarse chloritized and devitrified Tuffs 7c Coarse chloritized and devitrified Tuffs 7b
	Weathered quartz diorite/andesite F2	Chloritized and kaolinized quartz-rich coarse andesitw 8
	Lower Interbedded andesitic tuffs and tuffaceous andesites and trachytes F1	Coarse chloritized and devitrified Tuffs 7a Coarse hematitized chloritized andesite Tuffs 6a Coarse chloritized Andesite 5a Hematitized chloritized Andesite 4a Chloritized Andesite 3a Hematitized Chloritized and devitrified Tuffs 2a Chloritized and devitrified Tuffs 1a

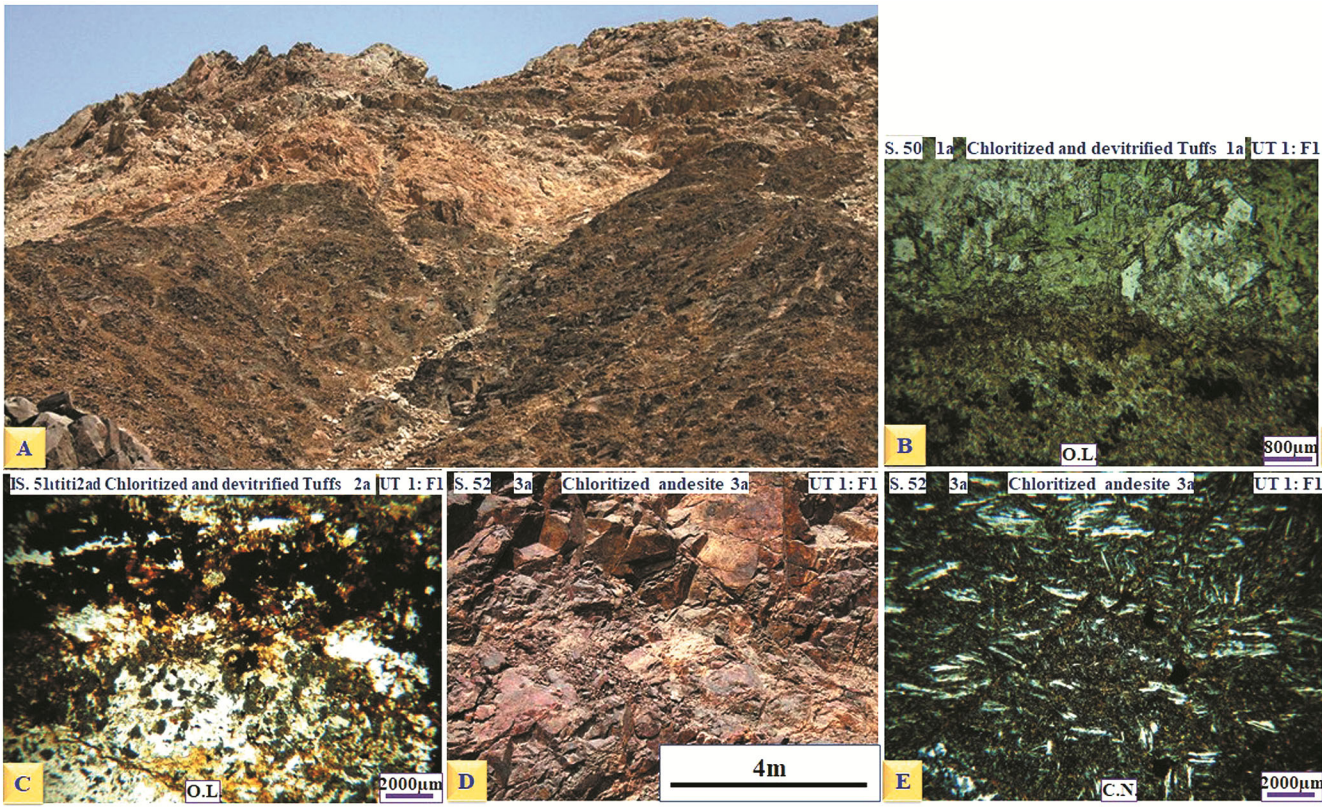

Fig. 5 — (A) Field photo show the interlayered volcaniclastic succession and the overlying marble units; (B) Chloritized and devitrified tuffs of the first volcaniclastic unit I (O.L. = Ordinary Light, C.N. = Crossed Nicols); (C) Hematitized Chloritized and devitrified Tuffs 2a that composed from laminated red and grey tuffaceous mudstone; (D) The chloritized andesite 3a composed from massive to layered chloritized andesite; and (E) The andesite is composed from lath-like simple twinned plagioclase show flow (trachytic) texture and embedded in chloritized and devitrified mudstone

Hematitized Chloritized and devitrified Tuffs 2a

Hematitized Chloritized and devitrified Tuffs 2a overlying type la (Fig. 3, Column B). It is present within an interval of 15 m thick and is composed of laminated red and grey tuffaceous mudstone (Fig. 5C). It consists of precursor tuffaceous mudstone of variable mineralogical composition and deposited under different depositional environments. This led to the formation of tuffaceous mudstone of chloritic and non chloritic composition. Diagenetic and metamorphic hematitization of the chloritic bands led to the formation of red iron oxyhydroxides and

hematite bands and laminae. The light bands are subjected to progressive diagenetic devitrification and formation of microcrystalline quartz.

Chloritized andesite 3a

Chloritized andesite 3a which represents the lower 9 m of column B of Figure 3. It is composed from massive to bedded chloritized andesite (Fig. 5D), of lath-like plagioclase embedded in chloritized and devitrified mudstone (Fig. 5E). The plagioclase crystals show orientation (flow) textures. In some domains, the rock is slightly crystalline and completely forms chloritized tuff. Some black goethite and hematite patches and domains are present within the chloritic matrix. Within this fine green chloritic matrix, large euhedral to subhedral chlorite flakes are observed (Fig. 6A). Some black hematite and goethite patches and domains are observed (Fig. 6A).

Hematitized chloritized andesite 4a

Hematitized chloritized andesite 4a attains up to 7 m thick in the middle part of the column B (Fig. 3). It consists mainly of hematitized chloritized andesite (Fig. 6B). The dark bands are composed of slightly hematitized and chloritized materials of amorphous tuffs and plagioclase crystals. The light color patches are composed from plagioclase laths and microcrystalline quartz.

Coarse chloritized andesites 5a

Coarse chloritized andesites 5a is present in the lower part of column C (Fig. 3). It consists of coarse chloritized andesite and trachyte. The plagioclase crystals are present in semi-oriented clusters and aggregates (Fig. 6C). The interstitial chloritized matrix is progressively hematitized giving rise yellowish brown Fe-oxyhydroxides and black goethite and hematite.

Coarse hematitized chloritized andesitic tuff 6a

Coarse hematitized chloritized andesitic tuff 6a which is of 10 m thick and consists of massive bedded reddish brown to black tuffs. Microscopically, it consists of light color plagioclase crystals of flow texture embedded in slightly hematitized chloritized matrix (Fig. 6D). The progress of hematitization processes led to the formation of reddish brown and black goethite and hematite (Fig. 6E).

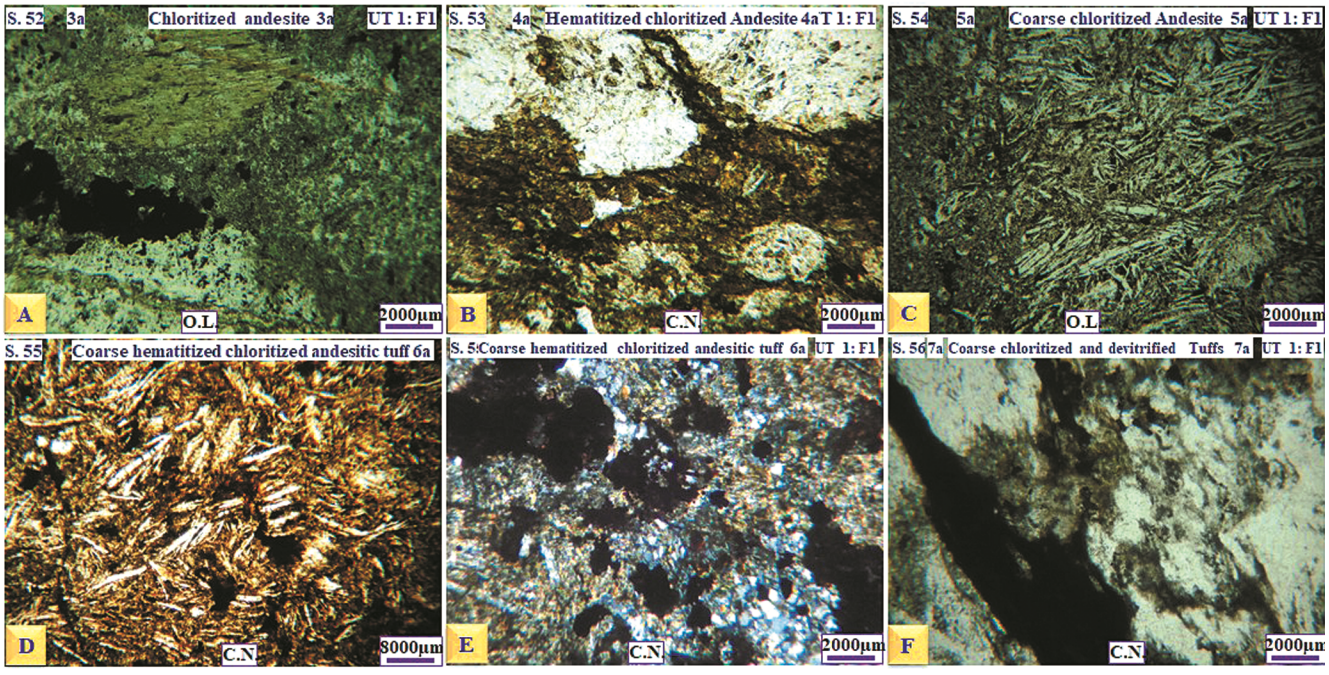

Fig. 6 — (A) Large euhedral to subhedral chlorite flakes are observed within this fine green chloritic matrix; (B) Hematitized chloritized andesite 4a which consists mainly from hematitized chloritized andesite. The light color patches are composed from plagioclase laths and microcrystalline quartz; (C) Coarse chloritized andesites 5a which consists of coarse chloritized andesite and trachyte. The plagioclase crystals are present in semi-oriented clusters and aggregates; (D) Light color plagioclase crystals of flow texture embedded in slightly hematitized chloritized matrix within type 6a; (E) The progress of hematitization processes and the formation of reddish brown to black goethite and hematite patches and domains with the formation of white color quartz domains; and (F) Coarse chloritized and devitrified tuff 7A which is composed from green tuffaceous mudstone which suffered from advanced stages of diagenetic chloritized and devitrification

Coarse chloritized and devitrified tuff 7a

Coarse chloritized and devitrified tuff 7a is present in the upper part of the column C (Fig. 3). It composed from green tuffaceous mudstone which suffered from advanced stages of diagenetic chloritized and devitrification (Fig. 6F). This resulted in the formation of white areas of microcrystalline quartz and dark green areas of chlorite.

Weathered quartz diorite/ andesite facies F2

Weathered quartz diorite/ andesite facies F2 is present in the lowermost part of column D (Fig. 3). It attains up to 2.5 m thick and composed from kaolinized quartz diorite/ andesite (Fig. 7A). It is highly fractured, massive and contains some black fresh patches and domains of quartz diorite/ andesite (Fig. 7A). It is composed from large green hornblende crystals embedded in microcrystalline quartz, the hornblende crystals show different stages of hematitization giving rise to reddish brown iron oxyhydroxides and hematite. Large black amorphous undevitrified tuffaceous patches are recorded. These white tuffaceous materials contain some hematitized patches and domains (Fig. 7B). Some white microcrystalline quartz patches are present within the large green hornblende patches.

Upper interbedded andesitic tuffs and tuffaceous andesites and trachytes F3

Upper Interbedded andesitic tuffs and tuffaceous andesites and trachytes F3 attains up to 90 m thick (Fig. 5). It comprises the following petrographic lithotype:

Coarse chloritized and devitrified tuff 7b

Coarse chloritized and devitrified tuff 7b consists of tuffaceous mudstone. It is composed of fine grained devitrified and slightly chloritized tuffaceous mudstone (Fig. 7C). Some black Fe-oxyhydroxides and hematite patches are observed within the green chloritic mudstone. These are formed in irregular domains of wavy and crenulated forms (Fig. 7C).

Coarse chloritized and devitrified tuffs 7c

Coarse chloritized and devitrified tuffs 7c is composed from black tuffaceous mudstone (Fig. 7D, E). It consists mainly of fine chloritized and devitrified tuffaceous mudstone (Fig. 7E). Some coarse crystalline white devitrified domains of microcrystalline quartz are present. These domains were formed during diagenetic recrystallization and metamorphic alteration of the fine dense tuffaceous materials. Some of these domains are chloritized (Fig. 7F) and the chlorite flakes are hematitized into blood red to black crystals.

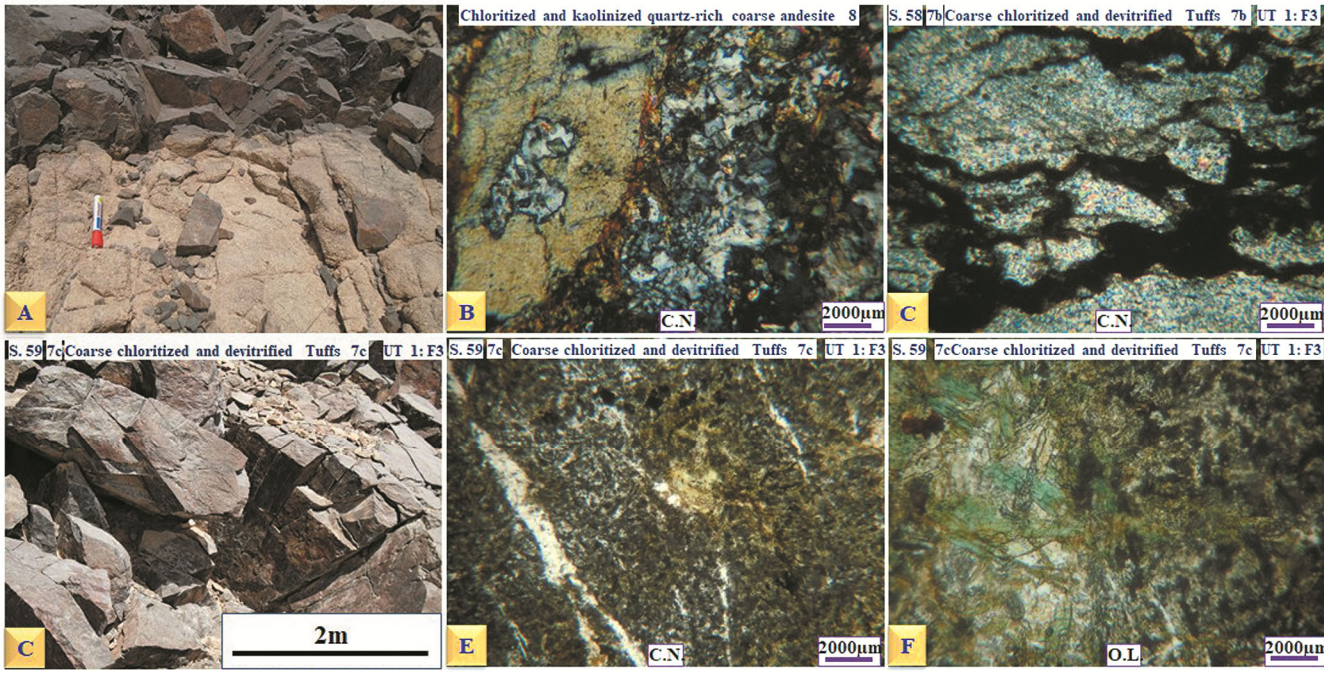

Fig. 7 — (A) Weathered Quartz Diorite/ Andesite Facies F2 which is highly fractured and massive and contains some black fresh unweathered patches and domains; (B) The hornblende crystals show different stages of hematitization giving rise to reddish brown iron oxyhydroxides and hematite with large black amorphous undevitrified tuffaceous patches; (C) Some black Fe oxyhydroxides and hematite patches and flasers are observed within the green chloritic mudstone; (D, E) Coarse chloritized and devitrified tuffs 7C which is composed from black chloritized and devitrified tuffaceous mudstone; and (F) Some coarse crystalline white devitrified domains of microcrystalline quartz that formed during diagenetic recrystallization of the fine dense tuffaceous materials

Chloritized and devitrified tuffs 1b

Chloritized and devitrified tuffs 1b is present in the uppermost part of the 1st volcaniclastic unit I (Fig. 4, column A). It is composed of devitrified and calcitized tuffs which are mottled and contains light white and dark grey patches and domains (Fig. 8A). Lath-like feldspar crystals are seen formed within the tuffaceous materials (Fig. 8B). These feldspar crystals vary in sizes and shapes (Fig. 8D). Some dark tuffaceous materials show progressive stages of degradation and alteration into microcrystalline clay minerals (mostly sericite and mica). During ultimate stages of alteration, large quartz crystals were formed in association with kaolinite and hydromica. Some green chlorite flakes become altered into yellowish brown flaky aggregates. The progresses of alteration processes led to the formation of red irregular and intersected flakes (Fig. 8C). This stage of alteration is associated with the formation of amorphous honey color of iron oxyhydroxides. This material contains interstitial relicts of slightly weathered (altered) chlorite. The processes of oxidation of chlorite are associated with the formation of microcrystalline quartz (Fig. 8D). Ultimate stages of hematitization led to the formation of homogeneous amorphous blood red iron-oxyhydroxide materials. This stage of alteration is accompanied with the formation of brown goethite and hematite shreds and veinlets.

Hematitized chloritized and devitrified tuffs 2c

Hematitized chloritized and devitrified tuffs 2c is represented by greyish white tuffaceous mudstone (Fig. 4, column A). It consists mainly of euhedral to subhedral undegraded tuffaceous materials embedded in completely degraded tuffaceous interstitial matrix. Some black undegraded relicts are still seen within the secondary formed clay minerals. In association with the black tuffaceous crystals, light lamellar twinned plagioclase, small green chlorite and hornblende crystals are present (Fig. 8E). Long simple twinned hornblende crystals are observed within the microcrystalline quartz devitrified matrix (Fig. 8E). These crystals are most probably formed instead of precursor simple twinned feldspar crystals (Fig. 8F). Some of the green flakes becomes progressively oxidized and hematitized giving rise to yellowish brown phase. The oxidation process is accompanied with the swelling and exfoliation of the precursor hornblende crystals and formation of iron oxyhydroxides interstratified with the resulted clay minerals. Ultimate stage of alteration led to the

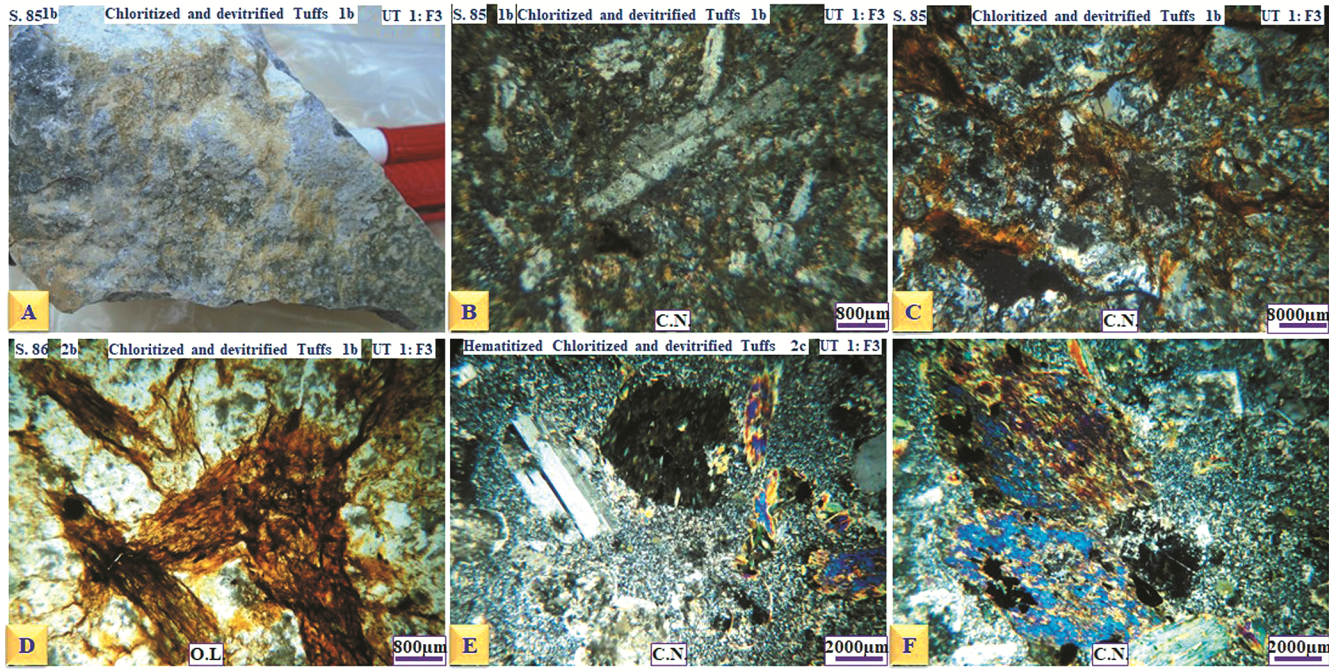

Fig. 8 — (A) Type 1b which is composed from devitrified and calcitized tuffs which is mottled and contains light white and dark grey patches and domains; (B) Light and dark domain with lath-like plagioclase crystals are seen formed with in the tuffaceous materials; (C) The progresses of alteration processes led to the formation of blood red irregular and intersected flakes contains interstitial relicts of slightly weathered (altered) chlorite; (D) This stage of alteration is associated with the formation of amorphous honey color of iron oxyhydroxides; (E) Type 2c, black tuffaceous crystals, light lamellar twinned plagioclase, small green chlorite and hornblende crystals are present; and (F) Long simple twined hornblende crystals are observed within the microcrystalline quartz devitrified matrix

formation of amorphous iron oxyhydroxides, clay minerals and quartz (Fig. 9A). Staining of the other unoxidized minerals by iron oxides led to the red color of this petrographic type.

Chloritized Andesite 3b

Chloritized Andesite 3b is present in the upper part of this unit (Fig. 4, Column B). It is represented by layered chloritized andesite and andesitic tuff in repeated cycles. Microscopically, it consists of fine crystalline rock of groundmass intersected zoned plagioclase crystals, and green hornblende flakes with less frequent quartz (Fig. 9B). Black crystals of iron oxides are also present within this fine groundmass. Large lamellar twinned plagioclase crystals are present. These crystals show incipient stages of chloritization. Light grey veinlets are present cross cutting the whole petrographic lithotype. White color devitrified patches of microcrystalline quartz are seen (Fig. 9C). These patches are slightly to completely chloritized (Fig. 9C).

Chloritized Andesite (meta-andesite) 3c

Chloritized Andesite (meta-andesite) 3c occurs at the topmost part of unit I (Fig. 4, upper part of column B). It is bedded and composed of chloritized andesite and tuffaceous andesitic tuff. It is composed from lath-like slightly chloritized plagioclase crystals embedded in chloritized matrix rich in black iron oxyhdroxides (Fig. 9D). Yellowish black patches formed instead of the original andesite composition by the oxidation of the green chloritic patches. The initial stages of oxidation of the precursor green chlorite are seen in Figure 9E. In this stage, the green color of the chlorite becomes altered into yellowish green swelled and exfoliated mineral phase. Progressive stages of oxidation led to the formation of red amorphous iron oxyhydroxides containing black goethite and hematite. Interstitial clay minerals mostly sericite and vermiculite are seen within the oxidized crystals due to metamorphism and alteration.

Chloritized Andesitic tuffs (Meta-tuff) 10a

Chloritized Andesitic tuffs (Meta-tuff) 10a is recorded in the upper most part of F3 (Fig. 4 column C). It is of greyish green color and is composed mainly of massive chloritized and desiccated tuffaceous mudstone (Fig. 9F). Light color euhedral and prismatic plagioclase crystals are seen within this fine groundmass (Fig. 9F). Small microcrystalline veinlets are observed cross cutting the fine tuffaceous materials.

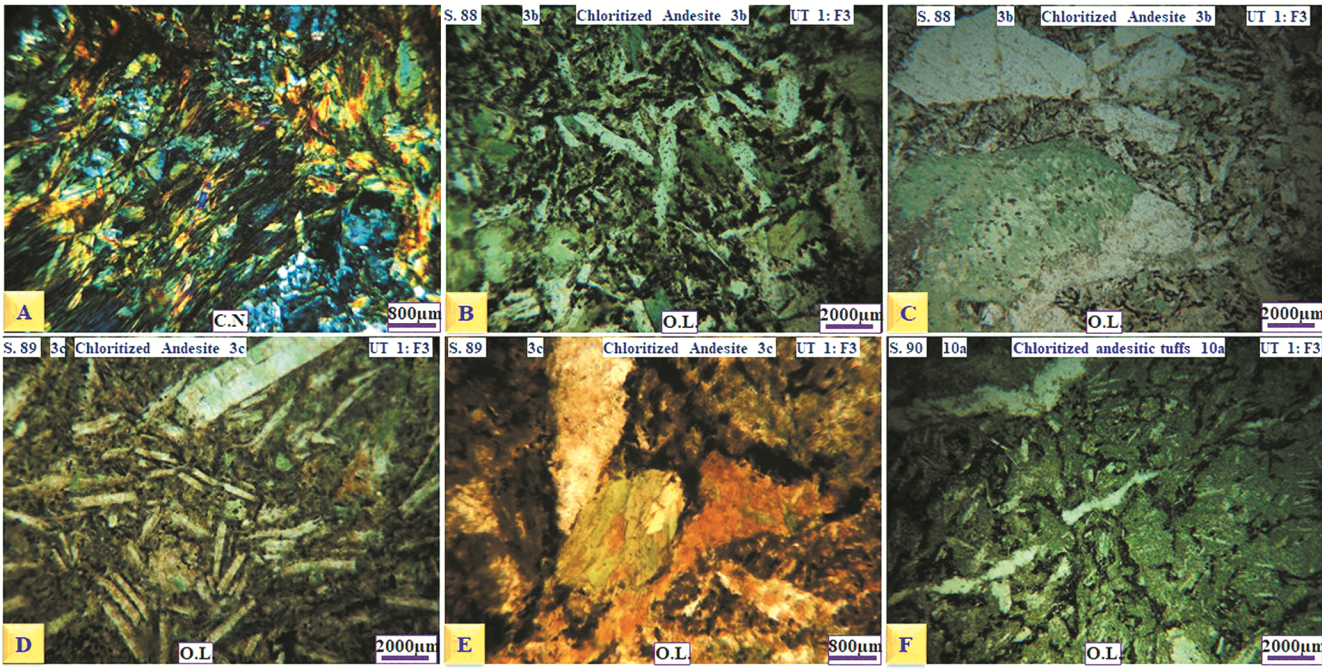

Fig. 9 — (A) Ultimate stage of alteration and the formation of amorphous iron oxyhydroxides, clay minerals and quartz; (B) Type 3b which consists of fine crystalline rock of groundmass intersected zoned plagioclase crystals, green hornblende flakes with less frequent quartz; (C) White color devitrified patches of microcrystalline quartz that are slightly to completely chloritized; (D) Lath-like slightly chloritized plagioclase crystals embedded in chloritized matrix rich in black iron- oxyhdroxides and oxide crystals and crystallites; (E) The green color of the chlorite becomes altered into yellowish green swelled and exfoliated minerals phase; and (F) Chloritized Andesitic tuffs 10a which is fine crystalline and it composed mainly from massive chloritized and desiccated tuffaceous mudstone with light color euhedral and prismatic plagioclase crystals are seen within this fine groundmass

Some large light color prismatic crystals are observed within the fine crystalline matrix. Some crystals show progressive stages of chloritization and formation of chlorite crystals pseudo-morph instead after the plagioclase crystals. Some white color microcrystalline quartz patches and domains are observed within the chloritic fine groundmass; they are subjected to progressive and subsequent stages of alteration and formation of amorphous red iron oxyhydroxides. Also, small black goethite and hematite patches are seen within the green chloritic matrix.

Depositional, Diagenetic and Metamorphic model

From the description of the different units and related facies of the Samran Group, we can conclude that, the studied basic and intermediate volcanics and related volcaniclastics represent deposition within oceanic environments of island arc situation. The succession of Samran Group shows evidence supporting its formation during successive periods of volcanic activities and sedimentation. These evidences include the presence of interlayered volcaniclastics and carbonate horizons. The volcaniclastic horizons support deposition during volcanic activities while the carbonate horizons indicate deposition during the cession of the volcanic activities. There is a characteristic lateral facies changes in the studied volcanoclastic succession. It resulted from subaqueous water-laid volcaniclastic constituents *i.e.* volcanic ash, and fine volcanic derivatives. Also, the lithologic characteristic of these volcaniclastics revealed their derivation by subaqueous reworking, transportation and redeposition of cooled and lithified volcanic materials formed during subsequent volcanic eruptions (Fig. 10A). Progressive deposition of the volcaniclastic materials and beginning of syn- and post-depositional diagenetic processes led to the formation of green chloritic clays instead of the precursor tuffaceous

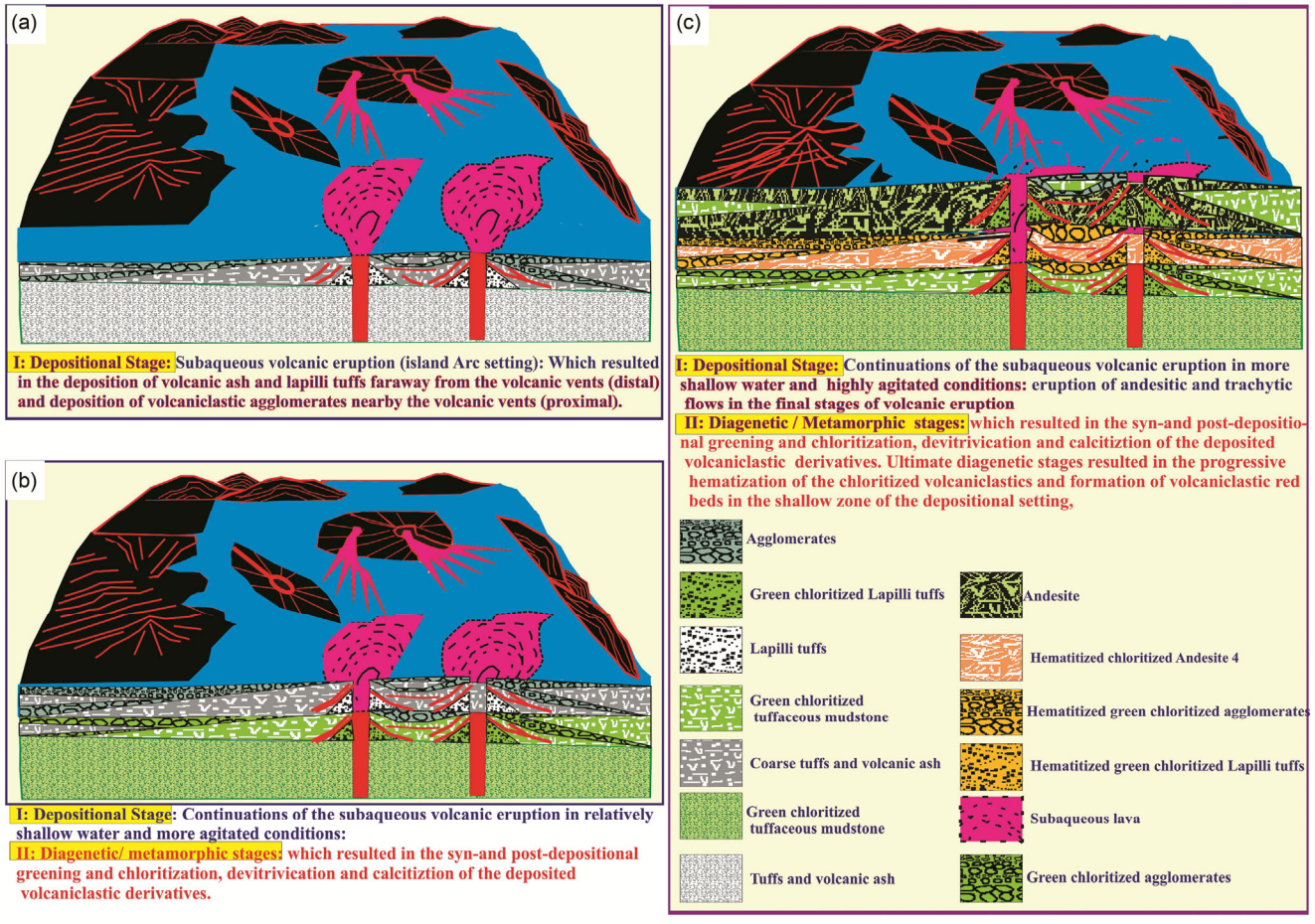

Fig. 10 — (A) Cross-section showing the subaqueous deposition of the volcaniclastic deposits in island arc setting; (B) I = The continuation of depositional stage of Fig. 10A; II = The diagenetic chloritization of the deposited volcaniclastic of stage 10A; and (C) I = The deposition of volcaniclastics in relatively shallow conditions; II = The continuation of the chloritization of the deposited volcaniclastic sediments and the hematitization of the chloritized volcaniclastic deposits

matrix and grains (Fig. 10B). During the progressive shoaling, the depositional environments became highly agitated and the deposited volcaniclastics become progressively chloritized and then hematitized giving rise to hematitic volcaniclastic beds (Fig. 10C). The formation of the hematite of the volcaniclastic red beds of wadi Halwate and Tayibit El Esm areas, Ablah district, Saudi Arabia, either by the direct hematitization of the tuffaceous materials specially in the oxidized depositional environments dominated in the upper parts of the shallowing-upward cycles or by the hematitization of the formed green celadonitic clays of the middle parts of the depositional cycles was concluded by Asaad & Mesaed[20] and Taj *et al.*[21].

Syn- and post-depositional authigenesis of green celadonitic clays in reducing environments is due to the high Fe^{2+}, Mg concentration, and the presence of Al and Si from the volcanic ash. The formation of green clays in marine environments was previously postulated[22-24]. The celadonitic clays are of different organic matter and Fe^{2+} content due to the variations in the physico-chemical conditions[20,25]. As a result of this lithologic variation, the green clays are subjected to different degrees of oxidation during the diagenetic and metamorphism processes.

Acknowledgments

The project was funded by the Deanship of Scientific Research (DSR), King Abdulaziz University, Jeddah, under grant no. G-335-145-1436. The authors, therefore, acknowledge with thanks DSR technical and financial support.

Conflict of Interest

Authors don't have any conflict of interest.

Author Contributions

AM, AS: the different stages of the field works, measurements of the detailed stratigraphic section, the petrographic description of the studied volcaniclastics. The depositional models and mineral paragenesis.

References

1 Fisher R V & Schmincke H U, *Pyroclastic rocks*, (Springer-Verlag, Berlin), 1984, pp. 472.

2 Cas R F & Wright J V, *Volcanic successions, Modern and ancient*, (Allen & Unwin, London), 1987, pp. 528.

3 Hargrove U S, Stern R J, Kimura J, Manton W I & Johnson P R, How juvenile is the Arabia-Nubian Shield? Evidence from Nd isotopes and pre-Neoproterozoic inherited zircon in the Bi'r Umq suture zone, Saudi Arabia, *Earth Planeta Sci Lett*, 252 (2006) 306-328.

4 Tang Z, Julià J, Zahran H & Martin Mai P, The lithospheric shear-wave velocity structure of Saudi Arabia: Young volcanism in an old shield, *Tectonophysics*, 680 (2016) 8-27.

5 Ba -battat M A & Hussein A A, Geology and mineralization of the Jabal Samran-Jabal Abu Mushut area, *J King Abdulaziz Univ, Earth Sci*, 6 (1983) 571–578.

6 Johnson P R, Andresen A, Collins A S, Fowler A R, Fritz H, *et al*., Late Cryogenian-Ediacaran history of the Arabian-Nubian shield: a review of depositional, plutonic, structural, and tectonic events in the closing stages of the northern East African Orogen, *J Afr Earth Sci*, 61 (2011) 167–232.

7 Nebert K, Geology of the Jabal Samran and Jabal Farasan region, *Saudi Arab Dir Gen Min Reso Bull*, 4 (1969) p. 32.

8 Skiba W J & Gilboy C F, Geology of the Rabigh-Khulays quadrangle, 22/39, Kingdom of Saudi Arabia, *Unpublished manuscript, Saudi Geo Surv (SGS) Library*, (1975) p. 597.

9 Schmidt D L, Hadley D G, Greenwood W R, Gonzalez L, Coleman R G, *et al.*, Stratigraphy and tectonism in the southern part of the Precambrian Shield of Saudi Arabia, *Saudi Arab Dir Gen Min Reso Bull*, 8 (1973) 13 p.

10 Smith C W & Kahr V, Geology of Jabal Samran, *Unpublished report*, *Saudi Arab Dir Gen Min Reso Bull, Jeddah, Saudi Arabia*, (1966).

11 Skiba W J, The form and evolution of late Precambrian plutonic masses in the Jiddah-Rabigh-Wadi Al- Quaha area, Saudi Arabia, In: *Evolution and Mineralization of the Arabian-Nubian Shield Cooray*, edited by Tahoun S A, *Inst App Geol Bull*, (Pergamon Press Ltd., Oxford), 3 (1980) 105–120.

12 Greenwood W R, Hadley D G & Schmidt D L, Tectono-stratigraphic subdivision of Precambrian rocks in the southern part of the Arabian Shield, *Geol Soc Am Abstracts Progr*, 5 (1973) p. 643.

13 Blodget H W & Brown G F, Geological Mapping by Use of Computer-Enhanced Imagery in Western Saudi Arabia, *US Geol Surv Profess Paper*, 1153 (1982) p. 10.

14 Johnson P R, Explanatory Notes to the Map of Proterozoic Geology of Western Saudi Arabia, *Saudi Geol Surv Techn Report SGS-TR*, 4 (2006) p. 62.

15 Roobol M J, Stratigraphic Control of Exhalative Mineralization in the Shayban Paleovolcanoes (22/39 A), *Saudi Arab Dep, Minis Min Resor Open-File Report DGMR-OF*, 10-7 (1989) p. 39.

16 Ramsay C R, Geologic map of the Rabigh quadrangle, sheet 22 D, Kingdom of Saudi Arabia, *Saudi Arab Dep, Minis Min Resor Geol Map GM*, 84 (1986) p. 49.

17 Pallister J S, Stacey J S, Fischer L B & Premo W R, Precambrian ophiolites of Arabia: Geologic setting, U-Pb geochronology, Pb-isotope characteristics, and implications for continental accretion, *Precam Rese*, 38 (1988) 1-54.

18 Stern R J, Johnson P R, Kröner A & Yibas B, Neoproterozoic ophiolites of the Arabian-Nubin shield, In: *Precam. Ophio. and Related Rocks*, edited by Kusky T M, (Elsevier), *Develop in Precam Geol*, 13 (2004) 95-128.

19 Moore T A & Ar-Rehaili H, Geologic Map of the Makkah Quadrangle, Sheet 21D, Kingdom of Saudi Arabia, *Saudi Arab Dep, Minis MinResor Map GM*, 107 (1989) p. 62.

20 Asaad M M & Mesaed A A, Origin and geochemistry of the Late Proterozoic intra-arc rift-related volcaniclastic red and green beds of Tayibit El Esm area, Ablah district, south central Arabian shield, Saudi Arabia, *Arab Jour Geosci*, 8 (2015) 7515–7536.

21 Taj R J, Mesaed A A, Moufti A, Qari M A T & Matsah M I, Origin and Diagenetic History of the fluvio-lacustrine/deltaic volcaniclastic red beds, W. Girshah-W. Halwate, Ablah district, Western Arabian Shield, Saudi Arabia, *5th Int Conf Geol Tethys Realm, South Valley Univ*, (2010) 227–248.

22 Mesaed A A, Stratigraphic setting and paleoenvironments of the Bartonian- Priabonian glaucony facies of the northern part of the Western Desert, Egypt, *Egypt J Geol*, 43 (2) (1999a) 1–27.

23 Mesaed A A, Origin and fabric evolution of the glaucony facies of the northern part of the Western Desert, Egypt, *Egypt J Geol*, 43 (2) (1999b) 29–54.

24 Mesaed A A & Surour A A, Mineral chemistry and mechanism of formation of the Bartonian glaucony of El Gedida Mine, El Bahariya Oases, Egypt, *Egypt Min*, 12 (2000) 1–28.

25 Mesaed A A, Mechanism of formation of the upper Eocene glauconitic ironstones and red beds of Jabal Qalamoon area, Western Desert, Egypt, *Egypt J Geol*, 48 (2004a) 17–44.